Ionospheric response to X-class solar flares in the ascending half of the subdued solar cycle 24

Rumajyoti Hazarika, Bitap Raj Kalita and Pradip Kumar Bhuyan*

Centre for Atmospheric Studies, Dibrugarh University, Dibrugarh 786 004, India.
**Corresponding author. e-mail: bhuyan@dibru.ac.in; pkbhuyan@gmail.com*

The signature of 11 X-class solar flares that occurred during the ascending half of the present subdued solar cycle 24 from 2009 to 2013 on the ionosphere over the low- and mid-latitude station, Dibrugarh (27.5°N, 95°E; magnetic latitude 17.6°N), are examined. Total electron content (TEC) data derived from Global Positioning System satellite transmissions are used to study the effect of the flares on the ionosphere. A nonlinear significant correlation (R^2 =0.86) has been observed between EUV enhancement (ΔEUV) and corresponding enhancement in TEC (ΔTEC). This nonlinearity is triggered by a rapid increase in ΔTEC beyond the threshold value $\sim$1.5 ($\times 10^{10}$ ph cm^{-2} s^{-1}) in ΔEUV. It is also found that this nonlinear relationship between TEC and EUV flux is driven by a similar nonlinear relationship between flare induced enhancement in X-ray and EUV fluxes. The local time of occurrence of the flares determines the magnitude of enhancement in TEC for flares originating from nearly similar longitudes on the solar disc, and hence proximity to the central meridian alone may not play the dominating role. Further, the X-ray peak flux, when corrected for the earth zenith angle effect, did not improve the correlation between ΔX-ray and ΔTEC.

1. Introduction

Solar flares abruptly emit large amounts of electromagnetic energy at a wide range of wavelengths, particularly X-ray and Extreme Ultra Violet (EUV), for a very short duration. Solar EUV and X-rays are the primary energy sources of ionisation in the earth's ionosphere. The sudden increase in X-ray and EUV fluxes during solar flares causes extra ionisation of the D, E and F regions of the earth's ionosphere in the sunlit hemisphere within short intervals of time. The solar EUV spectrum of the range 25–91 nm ionises the peak density region F of the ionosphere, while the soft X-rays with wavelengths less than 15 nm are responsible for the E region ionisation, and the Lyman-α ionises the D-region (Rishbeth and Garriott 1969). Solar flares may cause a sudden increase of total electron content (SITEC), short-wave fadeouts (SWF) and sudden D region absorption (SDA) (Donnelly 1971; Davies 1990; Liu *et al.* 1996, 2004, 2006). Many researchers have studied the effect of solar flares in the past and found that the earth's ionosphere in the sunlit hemisphere is significantly affected by solar flares (e.g., Mitra 1974; Davies 1990).

Earlier solar flare effects in the upper ionosphere were studied using ground-based measurements, such as ionosonde, incoherent scatter radar and HF wave propagation (e.g., Davies 1961; Thome and Wagner 1971; Davies and Donnelly 1966). However, these observations were limited in space or time resolution. With the arrival of space-based techniques, especially radio beacons, it became possible to examine the solar flare effects in the upper ionosphere in terms of total electron content (TEC), with high temporal and spatial resolution. For the

Keywords. X-class solar flare; EUV; TEC.

flares of 21 and 23 May, 1967, Garriott *et al.* (1967) were the first to identify a sudden increase of TEC due to solar flares in the upper ionosphere. They derived TEC values from ATS-1 satellite and found enhancement of 1–2 TECU (TECU = 10^{16} el m^{-2}) for the two flare events. The solar flare effect of the ionospheric F region was studied by VHF radio beacon experiment on geostationary satellites and TEC enhancement was noticed (Mendillo *et al.* 1974). Zhang and Xiao (2003) using GPS TEC measurements studied the ionospheric response to the great solar flare of 15 April 2001, for the whole sunlit hemisphere, and found maximum ∼2.6 TECU enhancement in TEC. They also found that the TEC enhancement reduces with increase in solar zenith angle of the flare. This result was in contrast to the earlier study by Mendillo *et al.* (1974), who found no correlation with TEC enhancement and solar zenith angle. The four most intense flares, one on 14 July 2000 and the other three on 28, 29 October 2003 and 4 November 2003 of solar cycle 23 have been studied with the GPS technique. Zhang and Xiao (2005) studied the morphological features of SITEC for the flare of 28 October 2003 and reported an enhancement of up to 14 TECU, depending upon the solar zenith angle during local noon time. Tsurutani *et al.* (2005) have reported that the comparatively less increase in TEC for the severest flare of 4 November 2003 was due to the limb location of the active region. The statistical analysis of solar flares by Le *et al.* (2013) showed that a limb flare has a smaller effect than a central flare on the ionosphere. They have explained that the main source of ionisation, EUV fluxes, can be absorbed by solar atmosphere due to a large central meridian distance (CMD), in the case of limb flare. Furthermore, they have observed that the CMD effect decreases with decreasing flare X-ray class. The solar flare EUV spectra has a strong centre to limb effects (Donnelly 1976). Zhang *et al.* (2002) showed that the solar EUV enhancement during flares correlates with the CMD value. Mahajan *et al.* (2010) observed that the enhanced peak TEC is highly correlated with the enhanced peak in EUV flux. They also found that the poor correlation with X-ray flux improved when the CMD of the solar flare location is considered. Zhang *et al.* (2011) have also shown that the correlation between ionospheric TEC enhancement and the soft X-ray peak flux in the 0.1–0.8 nm region is poor. They have explained that the flare location on the solar disc is an important parameter to determine the impact strength of the ionospheric TEC response to solar flares.

The sudden enhancements in solar irradiance during solar flare events can significantly change the density, temperature and composition in the earth's ionosphere. For improving the accuracy of the space weather prediction, and also for better understanding of the photochemical process, a study of the ionospheric variation with flare irradiance is necessary. However, due to the complexity

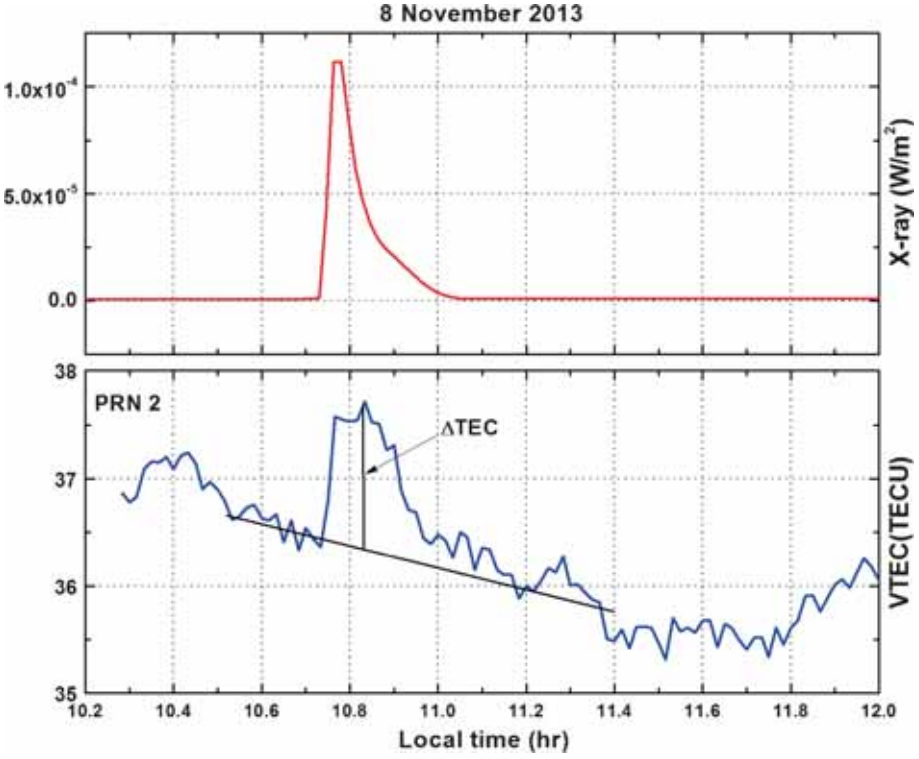

Figure 1. Method of estimation of ΔTEC.

or variety of flare responses observed over time and space, a comprehensive picture of the response of the ionospheric plasma to sudden solar flare burst has not yet emerged.

It is now known that the solar activity in the current solar cycle 24 preceded by an unusually deep minimum and is subdued in terms of activity, compared to solar cycle 22 and even 23. Therefore, the study of the effect of solar flares on the earth's ionosphere in this moderately active solar cycle might bring to light new response characteristics which have not been seen in the earlier highly active solar cycles. In the present study, TEC measured over Dibrugarh (27.5°N, 95°E, MLAT 17.6°N) using a GSV4004B GPS receiver has been utilised to examine the response of the ionosphere to 11 daytime X-class flares that occurred from the minimum to maximum of the current solar cycle 24. So far, to our knowledge, no report on the effect of all the solar flares that occurred during the ascending phase of the subdued solar cycle 24 on the ionosphere is available.

2. Data and method of analysis

Hitherto, there have been only 26 X-class flares during this rising half of solar cycle 24 (2009–2013). Out of these 26 X-class solar flares, 10 events occurred during night time (between 18 and 5 LT), TEC data are not available for four events, X5.4 and X1.3 occurred simultaneously on 7 March 2012 and therefore, only 11 events could be considered for this study. The GPS slant TEC data was recorded at a sampling rate of 60 seconds and then converted to the vertical TEC (VTEC), following the method described in Bhuyan and Hazarika (2013). The VTEC data from all the visible satellites with elevation mask of 50° was considered to minimise multipath effect. To quantify the variation of TEC due to solar flare, we calculated the background TEC values by drawing a baseline through the TEC before and after the flare. Then we calculated the enhanced TEC (ΔTEC) by subtracting this background value from the peak TEC value induced by the solar flares. The procedure for estimating the enhanced TEC (ΔTEC) is shown in figure 1. The vertical TEC (VTEC) for PRN2 on 8 November 2013 is shown during its corresponding X flare eruption. The black arrow indicates the estimated ΔTEC. The level of ionisation was quantified by calculating the % increase of TEC also, which is listed in table 1. The observed ΔTEC is supported by the time derivative of TEC, dTEC/dt = (TEC[i+1]−TEC[i]), where 'i' is the LT at a given instant of time for each satellite tracked. Examples of instantaneous enhancement of three X flare events of different magnitudes on 7 March

Table 1. *Selected X-class solar flare events with their peak fluxes (X-ray and EUV), locations, earth zenith angle (EZA) and flare time. The observed ionospheric effect from GPS TEC is listed here.*

Sl. no.	Date	Peak X-ray ($\times 10^{-4}$ W/m^2)	Peak EUV ($\times 10^{10}$ ph/cm^{2}s)	Flare location on the solar disc	Earth zenith angle (EZA) (degree)	Start time(LT)	End time(LT)	Peak time(LT)	Δ X-ray	ΔEUV	ΔTEC	% increase of TEC
1	07 03 2012	5.4	2.00	N17E29	71.3	06:35	06:73	06:57	5.35	3.23	4.92	14.04
2	14 05 2013	3.2	2.04	N12E81	68.47	06:32	08:33	07:44	3.19	0.25	1.59	06:21
3	15 02 2011	2.2	1.63	S21W14	62.62	08:17	08:29	08:19	2.29	2.98	3.45	13.14
4	24 09 2011	1.9	1.92	N13E59	70.75	15:54	16:21	16:13	1.87	2.13	1.78	03:21
5	23 10 2012	1.8	2.04	S10E56	53.08	09:46	09:54	09:50	1.80	2.07	1.71	04.71
6	25 10 2013	1.7	1.82	S08E73	66.7	14:26	14:56	14:34	1.72	0.11	0.6	00.99
7	13 05 2013	1.7	1.87	N11E89	60.03	08:26	09:05	08:49	1.73	0.11	1.22	03.84
8	22 09 2011	1.4	1.86	N09E89	73.35	16:52	18:17	17:34	1.46	0.16	0.77	01.79
9	08 11 2013	1.1	1.96	S11E10	48.48	10:53	11:02	10:59	1.10	0.28	1.57	03.99
10	05 03 2012	1.1	1.65	N18E55	47.95	09:03	11:16	10:38	1.07	0.13	0.47	00.89
11	19 11 2013	1.0	1.99	S13W66	74.19	16:47	17:17	16:59	1.02	0.09	0.47	00.64

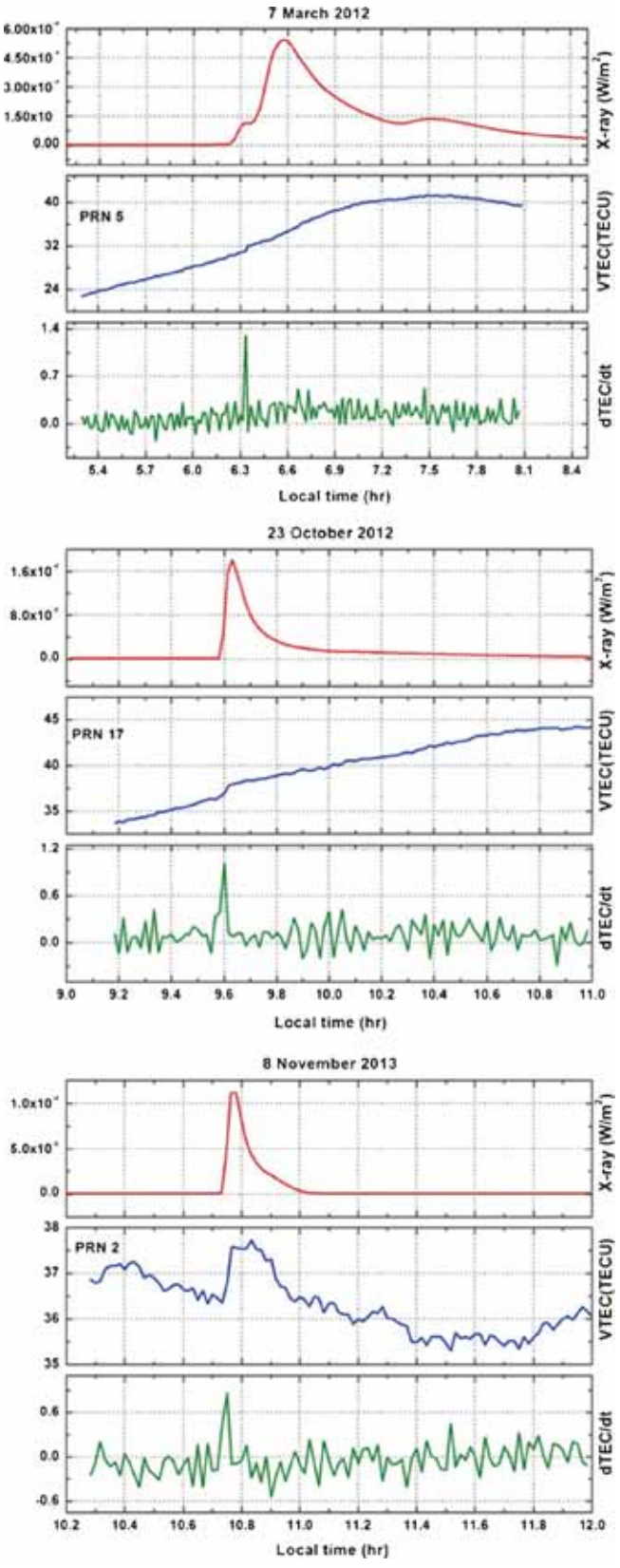

Figure 2. Representative curves showing the time rate of change of TEC for three different classes of X flare event on 7 March 2012, 23 October 2012 and 8 November 2013.

2012, 23 October 2012 and 8 November 2013 are shown with the X-ray flux intensity, in figure 2.

For the present study, the start time, peak time, end time and flare intensity of the solar flares provided by www.SolarMonitor.org were used. The active region maps of the Sun taken from the Mees Solar Observatory (http://www.solar.ifa.hawaii.edu/) were used. These maps provide the active region and its location on the visible hemisphere. The X-ray (0.1–0.8 nm) fluxes (in W/m^2) were obtained from the X-ray detectors onboard the Geostationary Operational Environment Satellite (GOES, http://spidr.ngdc.noaa.gov/spidr/) with 1-min frequency. The enhancement in X-ray (ΔX-ray) was calculated by taking the median of 60 min before the solar flare as a reference value of the X-ray flux, and then subtracting it from the peak X-ray flux during a solar flare. The EUV fluxes (ph cm^{-2} s^{-1}) were obtained from the Solar EUV Monitor (SEM) onboard the Solar and Heliospheric Observatory (SOHO) satellite. The SEM experiment presents the EUV flux in two spectral bands (26–34 nm and 0.1–50 nm). The 0.1–50 nm band has a lot of contribution from X-rays in it; therefore, for this study we have used only 26–34 nm band EUV data. The sampling rate of the EUV flux is 15 s. The 60 min median of the EUV flux before each solar flare was considered as the reference value, and then subtracting it from peak EUV during the flare, ΔEUV was obtained. The flare location on the solar disc is given by NOAA, Space Weather Prediction Centre. The solar zenith angle was taken from http://solardat.uoregon.edu/SolarPositionCalculator.html for the selected zone. The time format for all parameters is LT (= UT + 06:33 hr).

3. Results and discussion

Figure 3 illustrates the flare locations on the solar disc with active regions for the available eight flare events out of the total eleven events being investigated in this study. From figure 3, it is noticed that the central meridian distance (CMD) of the flare locations are largely different among the flares considered here. For example, the active region on 7 March 2012 was located at E29 longitude whereas the active regions corresponding to the 13 May 2013 and 22 September 2011 were located at E89 longitude. Table 1 lists the class, the location of the solar flares on the solar disc with start time, end time and peak time, peak X-ray and the EUV fluxes, ΔX-ray, ΔEUV, ΔTEC and %TEC enhancement for all the 11 flares considered here. It can be seen from table 1 that the selected flare events occurred within morning to afternoon hours.

Figure 4(a and b) shows the changes in X-ray and EUV fluxes for each of the 11 flares with corresponding changes in TEC for all visible GPS

satellites separately in local time. In both the figures, the green lines represent the TEC for different PRNs during the considered time and the red lines represent X-ray flux in figure 4(a), while in figure 4(b), the red lines represent the EUV flux. The peak times of enhancement X-ray and EUV flux for all flare events are not similar as seen in figure 4(a and b). The black arrow mark indicates the enhancement of TEC for different PRNs induced by the flare events. The observed magnitudes of enhanced TEC are different for different flare events. The processes and site of origin of the X-ray and EUV fluxes on the solar disc are not quite the same. The X-rays originate from the coronal active region of the solar disc while the EUV originates from a low-lying region of solar atmosphere (Bauer 1973). The EUV emissions suffer absorption in the solar atmosphere as it comes from low-lying regions. Thus flare originating from the limb region of the solar disc suffers more absorption than those at the central position of the solar disc. The time rate of change of TEC at the instant of peak enhancement is zero, and production is equal to loss, considering the little effect of transport within the short time interval of a flare effect on the ionosphere. Therefore, increase in the peak intensity of the EUV flux consequent to a flare determines the magnitude of the flare effect on the upper ionosphere. It is, therefore, necessary to examine the relationship between the X-ray fluxes and EUV fluxes to understand the response of TEC to X flares. Conflicting reports have emerged, regarding the relationship between X-ray and EUV fluxes. Horan *et al.* (1983) from an analysis of SOLRAD II satellite measurements of solar emissions in the soft X-ray band (0.1 to 0.8 nm plus 0.8 to 2.0 nm) and the EUV band (10–15 nm plus 70–103 nm) found a higher degree of correlations between the peak X-ray and EUV fluxes during X-class flares. On the other hand, Mahajan *et al.* (2010) from a study of 10 to 70 X-class flares found that the correlation between the

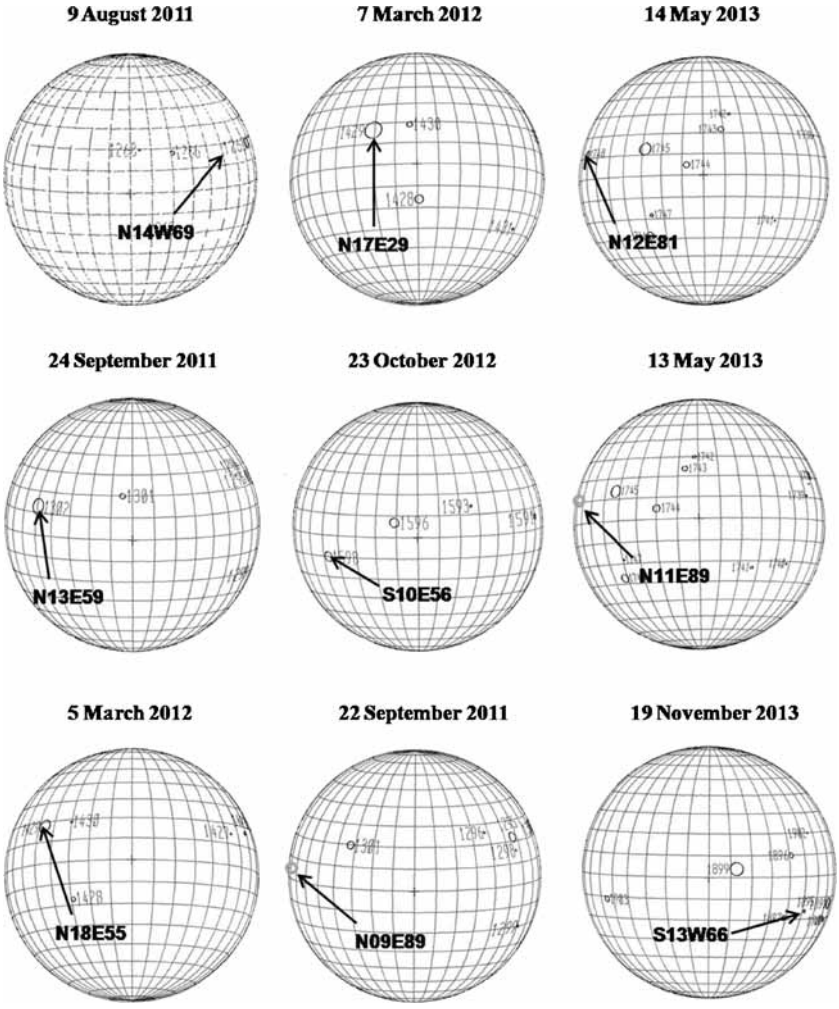

Figure 3. The active region maps of the Sun provided by the Mees Solar Observatory (http://www.solar.ifa.hawaii.edu/) for 9 days at the time of flare eruption (for the other three events images are not available). The arrow head points to the location of flaring active region on the solar disc.

peak X-ray flux and peak EUV flux is rather poor and intensity of X-ray flares is not an indicator of its effect on the upper ionosphere. However, the correlation improves significantly when the X-ray flux values are multiplied by cos (CMD), where CMD is the central meridian distance and provide a good indicator of EUV flux. They concluded that while examining solar flare effects in the upper ionosphere, one should relate these effects to EUV fluxes, and not to the raw value of X-ray flux. The relationship between the X-ray, EUV fluxes and TEC for 11 flares is examined and shown in figure 5. A nonlinear positive correlation ($R^2 = 0.47$) between ΔX-ray and ΔEUV is found in figure 5(a) with a second order polynomial best fit through the points. Rapid increase in X-ray flux beyond EUV flux enhancement of ∼1.5 ($\times$ 10^{10} ph cm^{-2} s^{-1}) gives rise to the observed nonlinearity between ΔX-ray and ΔEUV. The correlation obtained by fitting a linear regression line is much lower ($R^2 = 0.32$). Figures 5(b) and (c) are scatter plots of increase in TEC from the background (ΔTEC) with the corresponding enhancement in X-ray and EUV respectively. Figure 5(b) indicates a linear positive correlation ($R^2 = 0.68$) between ΔX-ray and ΔTEC, while the highest positive correlation ($R^2 = 0.86$) is obtained by fitting a 2nd order polynomial between ΔEUV and ΔTEC. Mahajan *et al.* (2010) have reported a linear positive correlation of ΔTEC with both peak X-ray ($r = 0.53$) and peak EUV ($r = 0.92$), while a nonlinear correlation of ΔTEC with peak EUV has been shown by Zhang *et al.* (2011). Higher correlation between EUV and TEC is expected, as EUV fluxes are primarily responsible for ionisation in the F region which contributes the most to TEC.

For a study of the effect of solar flare on the ionosphere, flare location is an important consideration. Afraimovich *et al.* (2002) observed that the increase in TEC during M-class flare was related to CMD as higher the CMD lower the increase in TEC, while Leonovich *et al.* (2010) found that this inverse relationship is valid for all three classes of flare (C, M and X). Mahajan *et al.* (2010) also found some evidence that SITEC is larger near the central meridian than at the limb. In figure 6, the

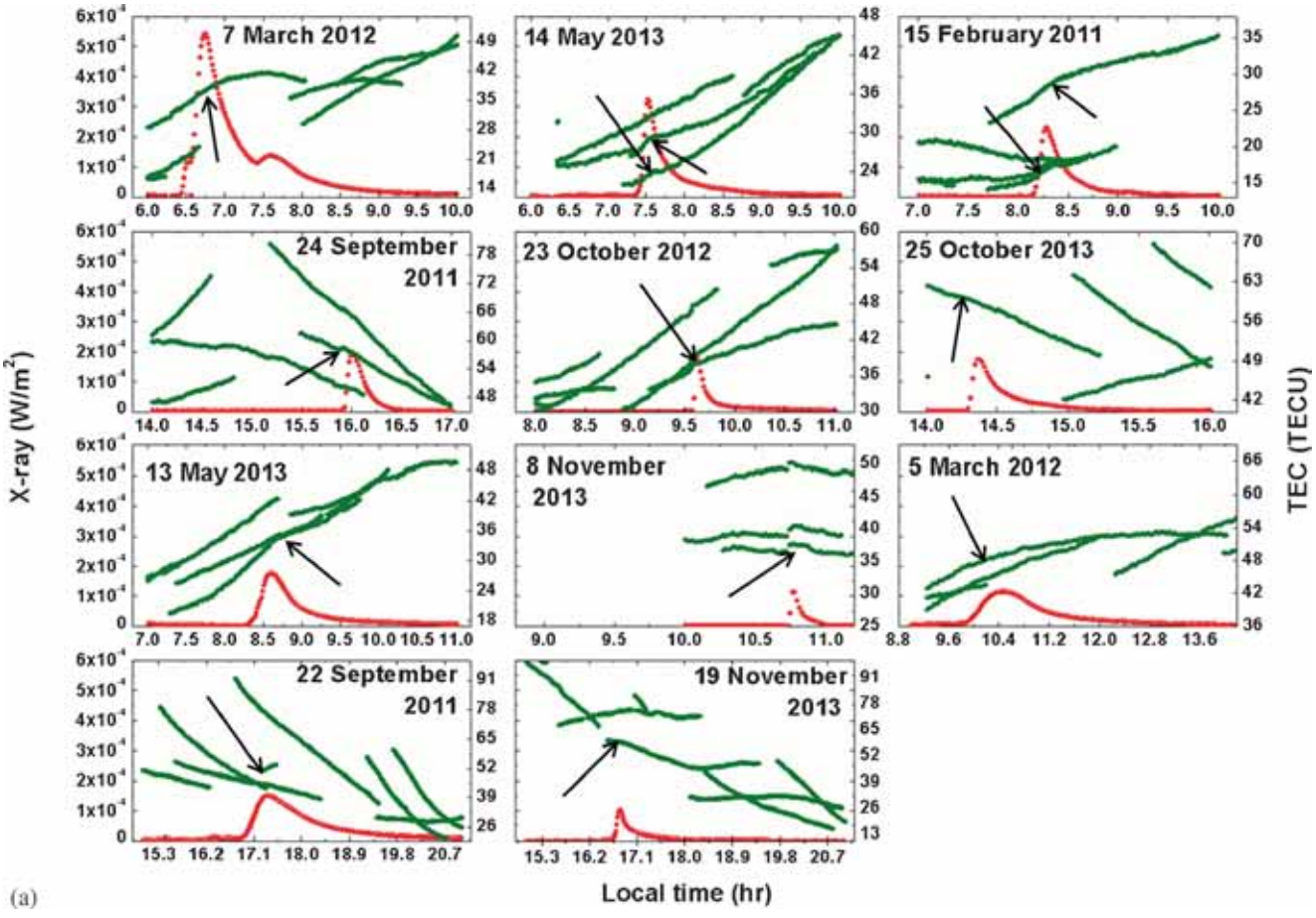

Figure 4. **(a)** The variations in X-ray (0.1–0.8 nm) (red line) and TEC against local time during 11 flare events. **(b)** The variations in EUV (26–34 nm) (magenta line) and TEC against local time during the 11 flare events. The green lines indicate the TEC for all visible satellites during the flare periods and arrow head indicates the enhancement of TEC during flare time.

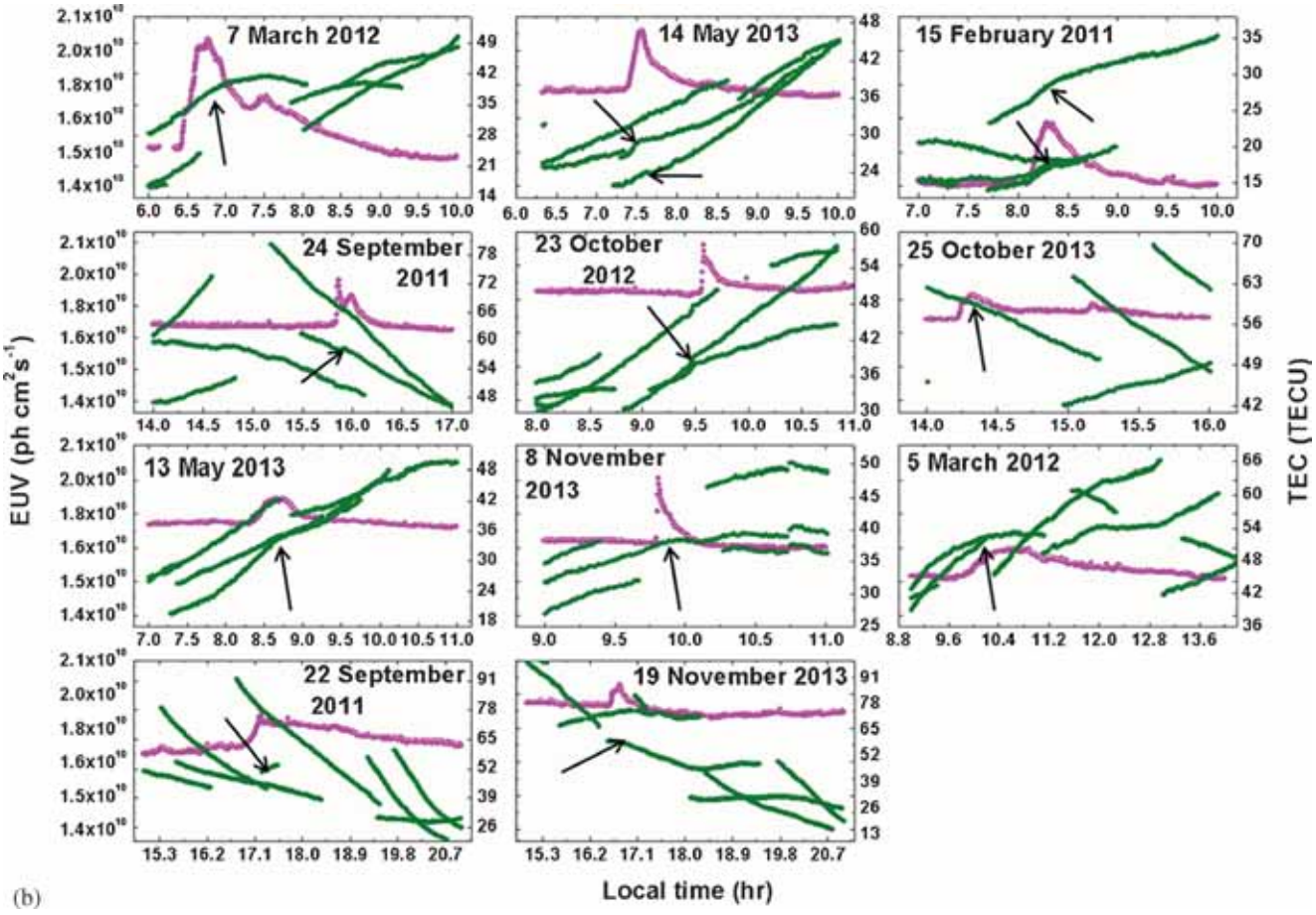

Figure 4. (*Continued.*)

correlation between the TEC enhancement and flare location on the solar disc is shown. The solid curved line is the best polynomial fit. It is seen from the figure that the amplitude of TEC enhancement increases towards the central meridian of the solar disc (low CMD), while it decreases for the flares at the near limb region (high CMD) of the solar disc. However, proximity to the central meridian may not play a dominating role in ionisation enhancement. The time of occurrence of the flare also determines the magnitude of enhancement for flares originating from nearly similar longitudes on the solar disc. The X5.4 flare of 7 March 2012 that occurred at 06:35 LT and peaked at 06:57 LT on 29E induced a 14% (4.92 TECU) enhancement in TEC. On the other hand, the flare of 8 November 2013 that occurred closer to the central meridian at E10 at 10:53 LT and peaked at 11:02 LT-induced a TEC enhancement of only 3.99% (1.57 TECU). The second highest enhancement of 3.45 TECU (13.14%) occurred at 08.19 LT due to the X2.2 flare that occurred on 15 February 2011 from 14W meridian.

According to Chapman ionisation theory (Chapman 1931), ionisation production exhibits a steady increase from about sunrise to noon, reaches a maximum and then falls to attain a minimum at sunset. To examine the relationship of TEC enhancement with the local time during the considered flare events, figure 7 is plotted. From table 1, it is noticed that none of the selected flares belong to the localnoon time. Out of 11, seven occurred during morning hours and other four during afternoon hours. The black solid curve in figure 7 stands for the second order polynomial best fit. From this figure, it is observed that the TEC enhancements during morning hours are larger than those in the afternoon hours. The plasma and hence the neutral temperature peaks in the sunrise hours, and falls gradually to a low level during mid-day and afternoon. Further, in a recent report, Kalita *et al.* (2015) have shown that the F2 peak height, hmF2, over Dibrugarh increases in the sunrise hours (06:00–08:00 LT), in all seasons. The morning flares are likely to accelerate the ion production rate due to rise in F peak height due to low recombination and high background temperature than that during the declining production phase in the afternoon. Zhang and Xiao (2000) also reported larger TEC enhancement in the morning than that in the afternoon at 15 GPS stations during an X9.4 solar flare.

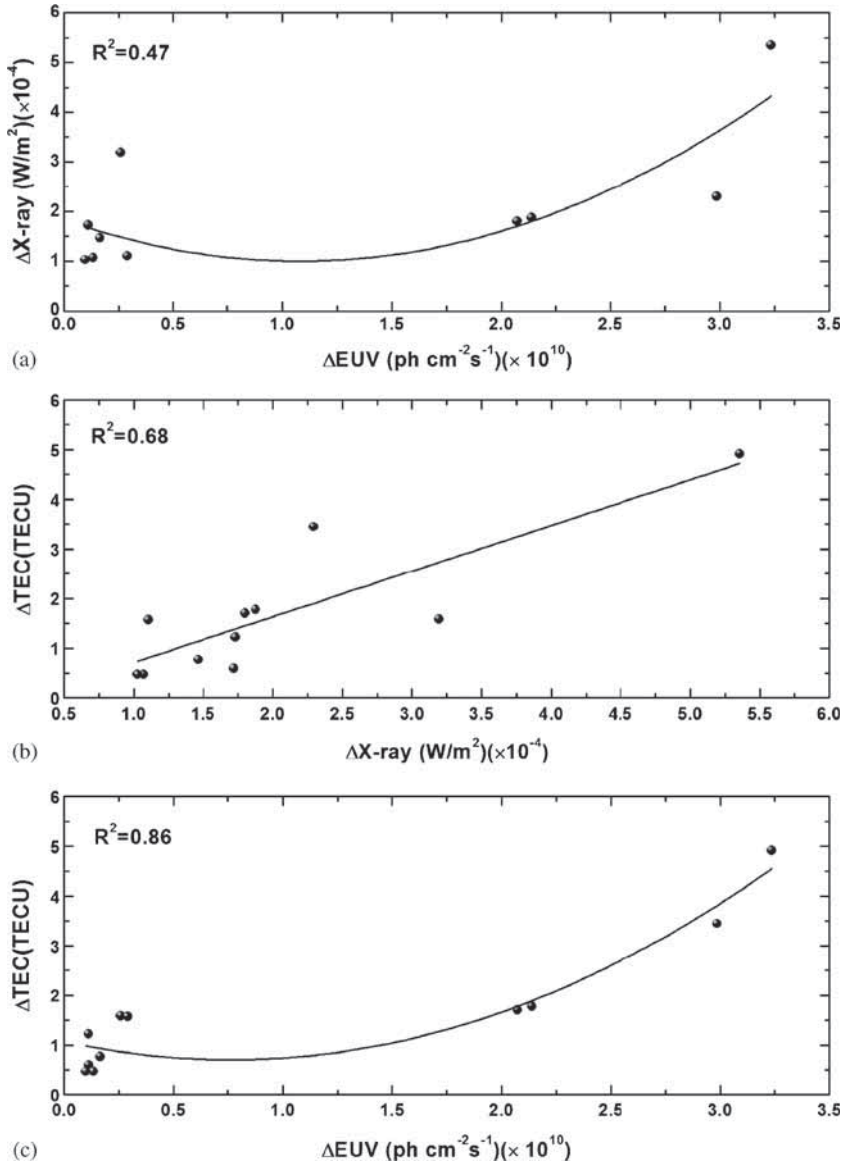

Figure 5. Scatter plot showing the correlation between (**a**) X-ray enhancement (ΔX-ray) and EUV enhancement (ΔEUV), **(b)** X-ray enhancement (ΔX-ray) and TEC enhancement (ΔTEC), **(c)** EUV enhancement (ΔEUV) and TEC enhancement (ΔTEC). The solid lines represent 2nd order polynomial best fit through the point in (a) and (c) and linear regression in (b).

Zhang *et al.* (2011) introduced an empirical formula (ImF = X-ray peak × cos (EZA)) for estimating the flare's impact on ionospheric TEC enhancement. Here, the earth zenith angle (EZA) represents the angle between the zenith direction of the flare location in the solar surface and the direction of the line of sight from the flare location to the earth. The correlation between ΔTEC and ImF for the selected flare events in the present study is shown in figure 8. The cosine of the EZA converts the observed flux to the real EUV flux reaching the earth's atmosphere or indirectly corrects the effect of CMD. It is seen from figure 8 that TEC enhancement exhibits a positive nonlinear correlation ($R^2 = 0.69$) with the factor ImF. Comparison with figure 5(b) indicates that the correlation did not improve when the X-ray flux intensity is corrected for the earth zenith angle. This is contrary to observations reported earlier by Mahajan *et al.* (2010) that when the peak X-ray flux is corrected for CMD effect, the correlation between TEC enhancement and X-ray flux increases significantly. Further, it is seen that for the selected 11 X-class flares, TEC enhancement increases, nonlinearly, with increase in ImF. However, Zhang *et al.* (2011) found a linear positive correlation between ΔTEC and ImF. It is already known that the solar zenith angle is an important factor for the ionisation of the upper atmosphere. For smaller solar zenith angles, the path length of solar radiation through the atmosphere is less, and hence ionisation intensity is more.

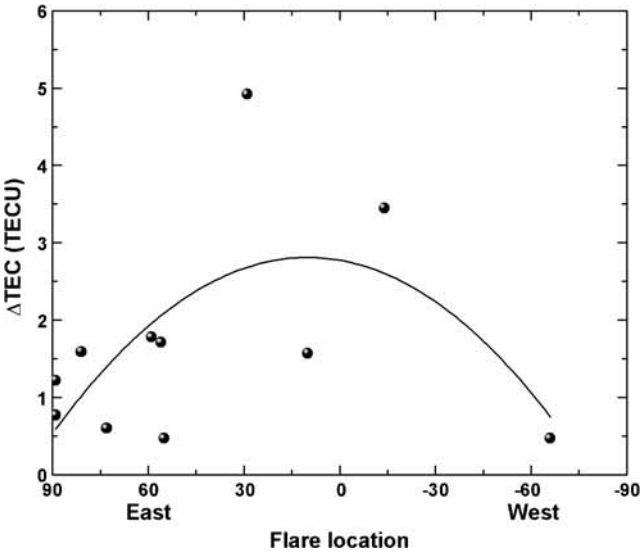

Figure 6. Scatter plot showing the relationship between the TEC enhancement (ΔTEC) and the flare location on the solar disc. The solid curve represents 2nd order polynomial best fit through the points.

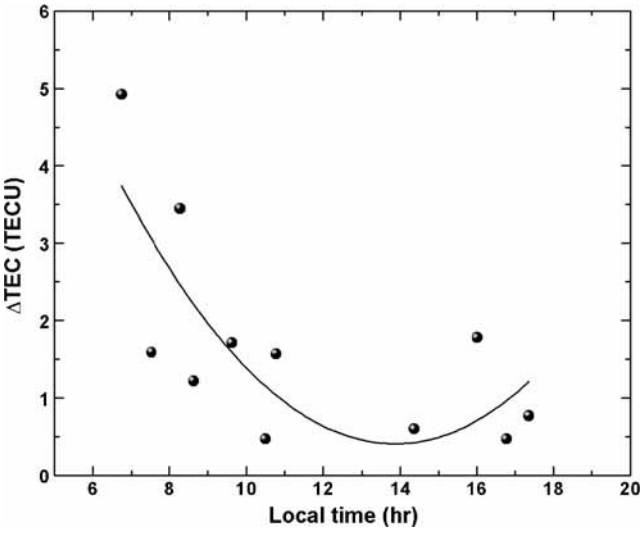

Figure 7. Scatter plot showing the relationship between enhancement in TEC and the local peak time of respective solar flares. The solid curve is the 2nd order polynomial best fit through the points.

4. Conclusions

An investigation is carried out on solar flare time electrodynamics and its influences on low mid-latitude ionosphere for X-class solar flare events, which occurred during the ascending half of the solar cycle 24. The solar flare effects on F region are investigated using TEC data. The results may be summarised as follows.

- EUV enhancement (ΔEUV) and corresponding enhancement in TEC (ΔTEC) show a non-linear significant correlation ($R^2 = 0.86$). This nonlinearity is triggered by a rapid increase in ΔTEC beyond the threshold value of ∼1.5 ($\times 10^{10}$ ph cm^{-2} s^{-1}), in ΔEUV.
- This nonlinear relationship between flare induced enhancement in X-ray and EUV fluxes is driven by a similar nonlinear relationship between X-ray and EUV flux.
- The local time of occurrence of the flares determines the magnitude of enhancement in TEC for flares originating from nearly similar longitudes on the solar disc, and hence proximity to the central meridian alone may not play the dominating role.
- Correction of the X-ray peak intensity for the earth zenith angle effect did not affect the correlation between X-ray and TEC enhancement.

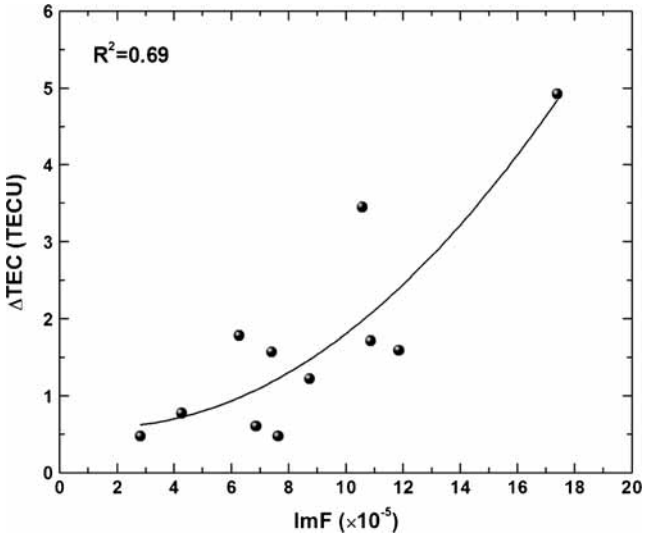

Figure 8. Relationship between enhancement in TEC (ΔTEC) and 'ImF' (i.e., the product of X-ray peak flux and the cosine of the earth zenith angle) of the solar flares. The solid curve is the polynomial best fit through the points.

Acknowledgements

This work was partially sponsored by the Indian Space Research Organisation (ISRO) through its Space Science Promotion Scheme (SSPS). We acknowledge the GOES, http://spidr.ngdc.noaa.gov/spidr/ and the Solar EUV Monitor (SEM) onboard the SOHO satellite for providing X-ray and EUV flux data. We are also thankful to the www.SolarMonitor.org for providing all information of the Sun, during solar flares. RH is grateful to the Department of Science and Technology, Government of India for providing fellowships under grant No. SB/S4/AS-127/2013. We are also grateful to the reviewers for their valuable comments and constructive suggestions.

References

Afraimovich E L, Altynsev A T, Grechnev V V and Leonovich L A 2002 The response of the ionosphere to faint and bright solar flares as deduced from global GPS network data; *Ann. Geophys.* **45** 31–40.

Bauer S J 1973 *Physics of Planetary Ionospheres*; Springer-Verlag, New York, Berlin.

Bhuyan P K and Hazarika R 2013 GPS TEC near the crest of the EIA at 95°E during the ascending half of solar cycle 24 and comparison with IRI simulations; *Adv. Space Res.* **52(7)** 1247–1260.

Chapman S 1931 Absorption and dissociative or ionising effects of monochromatic radiation in an atmosphere on a rotating Earth; *Proc. Phys. Soc. London* **43** 1047–1055.

Davies K 1961 Ionospheric effects associated with the solar flare of September 28, 1961; *Nature* **193** 763–764.

Davies K and Donnelly R F 1966 An ionospheric phenomenon associated with explosive solar flares; *J. Geophys. Res.* **71(11)** 2843–2845.

Davies K 1990 *Ionospheric Radio*; Peter Peregrinus, London.

Donnelly R F 1971 Extreme ultraviolet flashes of solar flares observed via sudden frequency deviations: Experimental results; *Sol. Phys.* **20(1)** 188–203.

Donnelly R F 1976 Empirical models of solar flare X-ray and EUV emission for use in studying their E and F regions effect; *J. Geophys. Res.* **81(25)** 4745–4753.

Garriott O K, da Rosa A V, Davies M J and Villard O G Jr 1967 Solar flare effects in the ionosphere; *J. Geophys. Res.* **72(23)** 6099–6103.

Horan D M, Kreplin R W and Dere P 1983 Direct measurements of the gradual extreme ultraviolet emission from large solar flares; *Sol. Phys.* **85(2)** 303–312.

Kalita B R, Bhuyan P K and Yoshikawa A 2015 NmF2 and hmF2 measurements at 95°E and 127°E around the EIA northern crest during 2010–2014; *Earth, Planets Space* **67(1)** 1–22.

Le H, Liu L, Chen Y and Wan W 2013 Statistical analysis of ionospheric responses to solar flares in the solar cycle 23; *J. Geophys. Res.* **118(1)** 576–582.

Leonovich L A, Tashchilin A V and Portnyagina O Y 2010 Dependence of the ionospheric response on the solar flare parameters based on the theoretical modeling and GPS data; *Geomag. Aeron.* **50(2)** 201–210.

Liu J Y, Chiu C S and Lin C H 1996 The solar flare radiation responsible for sudden frequency deviation and geomagnetic fluctuation; *J. Geophys. Res.* **101(A5)** 10,855–10,862.

Liu J Y, Lin C H, Tsai H F and Liou Y A 2004 Ionospheric solar flare effects monitored by the ground-based GPS receivers: Theory and observation; *J. Geophys. Res.* **109** A01307.

Liu J Y, Lin C H, Chen Y I, Lin Y C, Fang T W, Chen C H, Chen Y C and Hwang J J 2006 Solar flare signatures of the ionospheric GPS total electron content; *J. Geophys. Res.* **111** A05308.

Mahajan K K, Lodhi N K and Upadhayaya A K 2010 Observations of X-ray and EUV fluxes during X-class solar flares and response of upper ionosphere; *J. Geophys. Res.* **115** A12330.

Mendillo M, Klobuchar J A, Fritz R B, Darosa A V, Kersley L, Yeh K C, Flaherty B J, Rangaswamy S, Schmid P E, Evans J V, Schödel J P, Matsoukas D A, Koster J R, Webster A R and Chin P 1974 Behavior of the ionospheric F region during the great solar flare of August 7, 1972; *J. Geophys. Res.* **79(4)** 665–672.

Mitra A P 1974 *Ionospheric Effect of Solar Flares*; Norwell, Mass, D. Reidel.

Rishbeth H and Garriott O K 1969 *Introduction to Ionospheric Physics*; Academic Press, New York, London.

Thome G D and Wagner L S 1971 Electron density enhancements in the E and F regions of the ionosphere during solar flares; *J. Geophys. Res.* **76(28)** 6883–6895.

Tsurutani B T, Judge D L, Guarnieri F L, Gangopadhyay P, Jones A R, Nuttal J, Zambon G A, Didkovsky L, Mannucci A J, Iijima B, Meier R R, Immel T J, Woods T N, Prasad S, Floyd L, Huba J, Solomon S C, Straus P and Viereck R 2005 The October 28, 2003 extreme EUV solar flare and resultant extreme ionospheric effects: Comparison to other Halloween events and the Bastille Day event; *Geophys. Res. Lett.* **32(3)** L03S09.

Zhang D H and Xiao Z 2000 Study of the ionospheric TEC using GPS during the large solar flare burst on Nov. 6, 1997; *Chinese Sci. Bull.* **45(19)** 1749–1752.

Zhang D H, Xiao Z and Chang Q 2002 The correlation of flare's location on solar disc and the sudden increase of total electron content; *Chinese Sci. Bull.* **47(1)** 82–85.

Zhang D H and Xiao Z 2003 Study of the ionospheric total electron content response to the great flare on 15 April 2001 using the International GPS Service network for the whole sunlit hemisphere; *J. Geophys. Res.* **108(A8)** 1330.

Zhang D H and Xiao Z 2005 Study of ionospheric response to the 4B flare on 28 October 2003 using International GPS Service network data; *J. Geophys. Res.* **110** A03307.

Zhang D H, Mo X H, Cai L, Zhang W, Feng M, Hao Y Q and Xiao Z 2011 Impact factor for the ionospheric total electron content response to solar flare irradiation; *J. Geophys. Res.* **116** A04311.

MS received 21 December 2015; revised 22 May 2016; accepted 24 May 2016

Corresponding editor: K Krishnamoorthy